

Mast cells, macrophages, and crown-like structures distinguish subcutaneous from visceral fat in mice

Mehmet M. Altintas,* Adiba Azad,* Behzad Nayer,[†] Gabriel Contreras,* Julia Zaias,[§] Christian Faul,* Jochen Reiser,* and Ali Nayer^{1,*}

Department of Medicine* and Department of Pathology,[§] Leonard Miller School of Medicine, University of Miami, Miami, FL; and College of Engineering,[†] University of Miami, Coral Gables, FL

Abstract Obesity is accompanied by adipocyte death and accumulation of macrophages and mast cells in expanding adipose tissues. Considering the differences in biological behavior of fat found in different anatomical locations, we explored the distribution of mast cells, solitary macrophages, and crown-like structures (CLS), the surrogates for dead adipocytes, in subcutaneous and abdominal visceral fat of lean and diet-induced obese C57BL/6 mice. In fat depots of lean mice, mast cells were far less prevalent than solitary macrophages. Subcutaneous fat contained more mast cells, but fewer solitary macrophages and CLS, than visceral fat. Whereas no significant change in mast cell density of subcutaneous fat was observed, obesity was accompanied by a substantial increase in mast cells in visceral fat. CLS became prevalent in visceral fat of obese mice, and the distribution paralleled mast cells. Adipose tissue mast cells contained and released preformed TNF- α , the cytokine implicated in the pathogenesis of obesity-linked insulin resistance. **In summary, subcutaneous fat differed from visceral fat by immune cell composition and a lower prevalence of CLS both in lean and obese mice. The increase in mast cells in visceral fat of obese mice suggests their role in the pathogenesis of obesity and insulin resistance.**—Altintas, M. M., A. Azad, B. Nayer, G. Contreras, J. Zaias, C. Faul, J. Reiser, and A. Nayer. **Mast cells, macrophages, and crown-like structures distinguish subcutaneous from visceral fat in mice.** *J. Lipid Res.* 2011. 52: 480–488.

Supplementary key words obesity • insulin resistance • adipose tissue inflammation • mast cell • adipose tissue macrophage • crown-like structure • tumor necrosis factor- α

Over the past several decades a steady increase in the prevalence of obesity across the continents, especially in the US, has been observed (1). Increased caloric intake, mostly due to consumption of a high-fat diet, and decreased physical activity seem to be major contributors. Insulin resistance, hypertension, and dyslipidemia often accompany obesity. The constellation, referred to as metabolic syndrome,

is of grave consequence to human health. In fact, cardiovascular diseases, mostly as a result of long-standing metabolic dysregulations, are the leading cause of morbidity and mortality in many parts of the world.

The pathogenesis of obesity-linked insulin resistance is only partially understood. Accumulating evidence has revealed a strong association between obesity-linked insulin resistance and inflammation (2). Tumor necrosis factor- α (TNF- α), a prototypical pro-inflammatory cytokine, was upregulated in the epididymal fat of obese rodents, and neutralization of TNF- α ameliorated insulin resistance (3). Moreover, obese mice lacking TNF- α demonstrated improved insulin sensitivity (4). In addition, increased numbers of macrophages and their transcripts were reported in the epididymal fat of genetically and diet-induced obese (DIO) mice (5, 6). These adipose tissue macrophages (ATM) were found scattered between adipocytes (herein referred to as solitary ATM) or forming clusters around adipocytes. Based on ultrastructural and immunohistochemical alterations, it was argued that most ATM in obese mice and humans surround dead adipocytes, forming so-called crown-like structures (CLS) (7). Subsequently, we reported that CLS were distributed differentially in abdominal fat depots of DIO mice (8). Consistent with our findings, it was recently reported that CLS were also more prevalent in visceral than subcutaneous fat of leptin-deficient ob/ob and leptin receptor-deficient db/db mice (9).

Although macrophages are critical in innate and adaptive immunity, most immune responses are the result of interplay between multiple cell types and mediators of the immune system (10). Therefore, it comes as no surprise to learn that regulatory T cells (11), CD8⁺ effector T cells (12), natural killer T cells (13), and mast cells (14–16)

Abbreviations: ATM, adipose tissue macrophages; CLS, crown-like structures; DIO, diet-induced obesity; EAT, epididymal adipose tissue; HFD, high-fat diet; LFD, low-fat diet; MAT, mesenteric adipose tissue; PAT, perinephric adipose tissue; SAT, subcutaneous adipose tissue; TNF- α , tumor necrosis factor α .

¹To whom correspondence should be addressed.
e-mail: anayer@med.miami.edu

This work was supported by generous funds from the Katz Family Foundation. Manuscript received 15 September 2010 and in revised form 7 December 2010.

Published, JLR Papers in Press, December 9, 2010
DOI 10.1194/jlr.M011338

have also been implicated in the pathogenesis of obesity-linked insulin resistance. In addition to their role in host defense (17), mast cells are linked to inflammatory and autoimmune diseases, such as allergic reactions (18), bullous pemphigoid (19), multiple sclerosis (20), inflammatory arthritis (21), and atherosclerosis (22).

Once believed to solely provide structural support and serve as reservoir for energy surplus, adipose tissues are shown to regulate metabolism, blood pressure, immune responses, coagulation, and the function of other endocrine organs (23). However, not all fat is the same (24–26). Whereas visceral adiposity is associated with an increased risk for metabolic dysregulations and cardiovascular diseases, increased subcutaneous fat, especially around thighs and hips, appears to pose little or no risk. Visceral fat is found in association with internal organs. In the abdominal cavity, for example, there are omental, mesenteric, and perinephric adipose tissues. Due to its small size, the omentum in the mouse is much less studied than its counterpart in humans. However, epididymal adipose tissue is well developed in the mouse and is widely used in metabolic studies. Considering structural, functional, and biological differences between subcutaneous and visceral fat, we asked whether subcutaneous fat differs from visceral fat by the distribution of mast cells, solitary ATM, and CLS in lean and DIO mice.

RESEARCH DESIGN AND METHODS

Experimental animals

Animal care was in accordance with guidelines at the University of Miami. Male C57BL/6 mice were purchased from Taconic (Hudson, NY) and acclimated for two weeks before the beginning of the study. Mice were randomized to either a high-fat diet (HFD, 5.24 kcal/g, 60% of calories from fat) or a low-fat diet (LFD, 3.85 kcal/g, 10% of calories from fat) at the age of six weeks and were euthanized when they were six months old. Experimental diets were purchased from Research Diets, Inc. (New Brunswick, NJ). Mice were weighed with a Scout Pro balance SP202 (Ohaus, Pine Brook, NJ).

Glucose and insulin measurements

After overnight fasting (15 h), blood was sampled from the tail of unanesthetized mice. Blood glucose concentrations were measured using a Contour glucometer (Bayer, Tarrytown, NY). An enzyme-linked immunosorbent assay was used to measure serum insulin concentrations according to manufacturer's directions (Crystal Chem, Downer Grover, IL).

Histology

Tissues were fixed in Carnoy's fixative and embedded in paraffin. Five micron-thick sections were cut, baked at 60°C for 1 h, deparaffinized in xylene, rehydrated in a graded ethanol series, and then stained. Hematoxylin and eosin staining was performed with Harris' hematoxylin (Surgipath, Richmond, IL) for 30 s and eosin (Surgipath) for 2 min. Toluidine blue staining was carried out by briefly submerging tissue sections in 0.1% aqueous toluidine blue (EMS, Hatfield, PA) (27). Mast cells, solitary ATM, and CLS were counted in 20 high-power fields (400×), and their density was expressed as cells or CLS per mm² of tissue section. Light microscopic images were acquired using a Leica DMLB microscope with Leica DFC420 C color camera.

Enzyme histochemistry

Esterase activity of mast cells was detected using a technique developed by L. D. Leder with minor modifications (28). Briefly, tissue sections were incubated for 10 min with a mixture of new fuchsin acid solution (Poly Scientific, Bay Shore, NY), 4% sodium nitrite solution (Sigma-Aldrich), and naphthol AS-D chloroacetate solution (Sigma-Aldrich) in 0.1 M sodium phosphate buffer, pH 7.6 (EMS). The sections were then washed with distilled water, counterstained briefly with Mayer's hematoxylin (EMS), washed again with distilled water, dehydrated, and mounted with Cytoseal 60 (EMS).

Fluorescence staining

Staining of tissue sections with FITC-conjugated avidin was carried out as previously described (29). Briefly, deparaffinized tissue sections were incubated with a 1:200 dilution of FITC-conjugated avidin (BD Pharmingen, San Jose, CA) for 60 min followed by nuclear staining with DAPI (0.1 µg/ml) (Molecular Probes, Eugene, OR) for 5 min. TNF-α staining was performed using a polyclonal rabbit anti-serum (1:250 dilution) (Abcam, Cambridge, MA) for 1 h. Alexa Fluor 594 goat anti-rabbit IgG (1:1,000 dilution) (Molecular Probes, Eugene, OR) was used to detect the antibody against TNF-α. The stained sections were then mounted with Ultramount (Dako, Carpinteria, CA).

Confocal microscopy

Confocal images were acquired on a Zeiss LSM510/UV Axiovert 200M confocal microscope. A Zeiss plan-neofluar 40×/1.3 NA lens with Argon 351/364 nm laser for DAPI (blue, pinhole 3 Airy units), Argon ion 488 nm laser for fluorescein (green), HeNe543 laser for Alexa Fluor 594 dye (red), and reflected light (no detection filter) images (pinhole 1 Airy unit, 0.7 µm optical slice thickness) were used in single planes. Most images were acquired with 4-frame average. Simultaneous transmitted light images were acquired using the ChD detector, with the condenser adjusted for Koehler illumination, and contrast was adjusted using ChD detector gain and offset. Images were zoomed to 1×, 1.8×, 2×, 3×, 4×, or 5× using the confocal scanner optical zoom.

Electron microscopy

Adipose tissue was fixed by immersion in 2% glutaraldehyde and 2% paraformaldehyde in 0.1 M phosphate buffer, pH 7.4. The tissue was washed with buffer and postfixated in 1% osmium tetroxide in 0.1 M phosphate buffer for 2 h at 4°C. Samples were then rinsed in buffer, dehydrated in a graded acetone series, and infiltrated and embedded in Spurr's epoxy resin. Tissue sections were cut at 50 nm (Reichert Ultracut S microtome), retrieved onto 300 mesh copper grids, and contrasted with uranyl acetate and lead citrate. Sections were examined using a Morgagni 268 transmission electron microscope, and images were acquired with an AMT Advantage 542 CCD camera system.

F4/80 immunohistochemistry

After quenching endogenous peroxidase activity with 3% hydrogen peroxide, antigen retrieval was carried out in 10 mM citrate buffer, pH 6.0, using a digital decloaking chamber (Pacific Southwest Lab Equipment, Vista, CA). Tissue sections were blocked with 1.5% rabbit serum and then incubated with F4/80 antiserum (1:100) (AbD Serotec, Raleigh, NC). After incubation with an appropriate secondary antibody (1:200) (Vectastain Elite ABC kit, Vector Laboratories, Burlington, CA), sections were exposed to Avidin-Biotin Complex, developed using 3,3'-diaminobenzidine as substrate (Sigma-Aldrich, St. Louis, MO), and counterstained with Gill's Hematoxylin (Fisher Scientific, Pittsburgh, PA). All

incubations took place in a humid chamber at room temperature. Sections were rinsed with PBS between incubations.

Statistics

Values are shown as mean \pm SEM. Unpaired Student's *t*-test was used to assess statistically significant differences between groups of two. Comparisons between multiple groups were carried out using one-way ANOVA (ANOVA) with Bonferroni adjustment. GraphPad Prism software (5.0a) was used for calculations (GraphPad Software, La Jolla, CA).

RESULTS

Mast cells, solitary ATM, and CLS were demonstrated in abdominal fat depots of lean and DIO mice

After overnight fasting, HFD-fed mice ($n = 10$) demonstrated a higher body weight (48.7 ± 1.0 versus 36.7 ± 0.7 g), blood glucose (152 ± 13 versus 77 ± 6 mg/dl) and serum insulin (2.295 ± 0.197 versus 0.612 ± 0.078 ng/ml) concentrations, and HOMA-IR (25.3 ± 3.7 versus 3.4 ± 0.6) than LFD-fed mice ($n = 10$) (Fig. 1A–D). In the present study, the following fat depots were examined: epididymal, perinephric, mesenteric, and inguinal subcutaneous (Fig. 1E). Mast cells were rather inconspicuous in hematoxylin and eosin-stained tissue sections (Fig. 2A–C). When stained with toluidine blue, a basic aniline dye, mast cells were readily identified as cells with ample cytoplasm packed with large purple granules (27) (Fig. 2D–F). Mast cells contain a host of preformed, biologically active substances that are stored in cytoplasmic granules (17). The esterase activity of mast cells was demonstrated with naphthol AS-D chloroacetate as substrate (28) (Fig. 2G–I). Avidin, a basic glycoprotein, binds mast cell granules with high affinity and specificity (29). Fluorescein-conjugated avidin was also used to demonstrate mast cells (Fig. 2J–L). At the ultrastructural level, mast cells contain membrane-bound, electron-dense granules and occasional mitochondria in the cytoplasm (30). ATM were identified by immunohistochemical staining for the murine F4/80 antigen (Fig.

2M–O). A 160 kDa cell surface glycoprotein, F4/80 antigen is a specific marker for murine macrophages and is constitutively expressed at high levels in most macrophages (31). ATM were found either scattered between adipocytes (solitary ATM; Fig. 2M) or forming clusters enveloping adipocytes (CLS; Fig. 2N, O).

Mast cells are distributed differentially in abdominal fat depots

Mast cells were found in all four abdominal fat depots in lean and obese mice (Fig. 3). Their density, however, differed from one depot to another (Fig. 3A–J). In lean mice, the density of mast cells was the highest in subcutaneous fat compared with epididymal ($P < 0.01$), mesenteric ($P < 0.05$), and perinephric fat (Fig. 3A–E). In obese mice, however, the density of mast cells was higher in visceral than in subcutaneous fat (Fig. 3F–J). For example, mast cells were 15-fold more prevalent in epididymal than in subcutaneous fat. Of note, there was no statistically significant change in the density of mast cells in subcutaneous fat between lean and obese mice (Fig. 3K). However, mesenteric fat in obese mice contained 7-fold more mast cells than in lean mice (Fig. 3L). Mast cells were 24-fold more prevalent in perinephric fat in obese than in lean mice (Fig. 3M). With 90-fold increase, the largest change in mast cell density was seen in epididymal fat (Fig. 3N–P). Ultrastructural examination revealed mast cells packed with electron-dense granules and macrophages in connective tissues between adipocytes (Fig. 3Q, R). Immunofluorescence staining and confocal microscopy demonstrated that a subset of mast cells in the epididymal fat of obese mice expressed TNF- α (Fig. 3S–U). TNF- α was also present in granules adjacent to degranulating mast cells (Fig. 3V–X).

In lean mice, subcutaneous fat contained fewer solitary ATM than epididymal and perinephric fat

With respect to macrophages, large numbers of solitary ATM were present in abdominal fat depots of lean mice (Fig. 4). Subcutaneous fat, however, contained fewer solitary

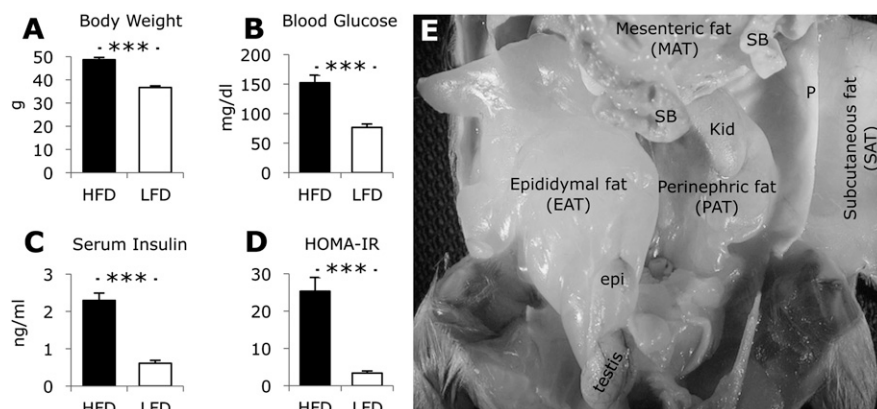


Fig. 1. Glucose homeostatic parameters and abdominal fat depots. Fasting body weight (A), blood glucose (B) and serum insulin (C) concentrations, and HOMA-IR (D) of C57BL/6 mice fed on a low-fat diet (LFD, \square) or a high-fat diet (HFD, \blacksquare) are shown ($n = 10$ in each group). Subcutaneous (SAT), mesenteric (MAT), perinephric (PAT), and epididymal (EAT) adipose tissues of a male mouse are demonstrated in vivo (E). epi, epididymis; kid, kidney; P, peritoneum; SB, small bowels. Data are expressed as means \pm SEM. *** $P < 0.001$.

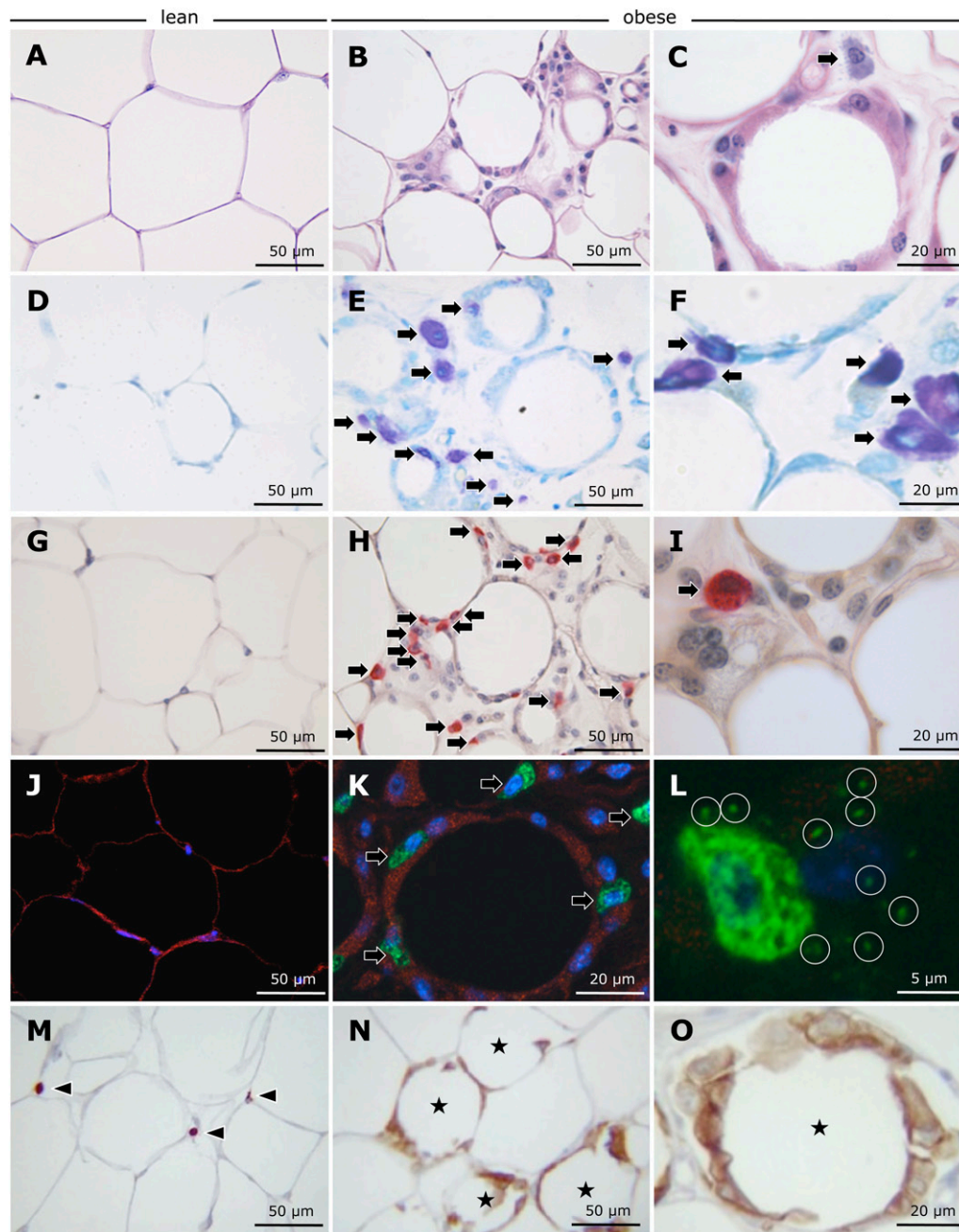


Fig. 2. Mast cells, solitary ATM, and CLS in adipose tissues. Mast cells (arrows) are shown in the epididymal fat of lean (left column) and obese (middle and right columns) C57BL/6 mice. Tissue sections were stained with hematoxylin and eosin (A-C), toluidine blue (D-F), naphthol AS-D chloroacetate (G-I), and fluorescein-labeled avidin (J-L). The latter was counterstained with DAPI to demonstrate nuclei (blue) and was examined under a confocal microscope. As evidenced by the presence of extracellular granules (circles), a mast cell in the process of degranulation is shown (L). Immunohistochemical staining for F4/80 identified solitary ATM (arrowheads) and CLS (stars) (M-O). Solitary ATM were found scattered between adipocytes (M). CLS consist of several macrophages surrounding adipocytes. (N-O). Scale bars as indicated. ATM, adipose tissue macrophages; CLS, crown-like structures.

ATM than perinephric ($P < 0.01$) and epididymal fat (Fig. 4A–E). Similarly, mesenteric fat contained fewer solitary ATM than perinephric ($P < 0.001$) and epididymal fat ($P < 0.01$) (Fig. 4A–E). Solitary ATM outnumbered mast cells in all four abdominal fat depots studied (Fig. 4F, G). The difference was 301-fold for epididymal, 156-fold for perinephric, 35-fold for subcutaneous,

and 33-fold for mesenteric fat depot (Fig. 4H). Certain regions of fat depots in obese mice contained large numbers of CLS (see below). As a result, the distinction between solitary ATM and those macrophages that participated in the formation of CLS became less distinct. Therefore, we elected not to enumerate solitary ATM in obese adipose tissues.

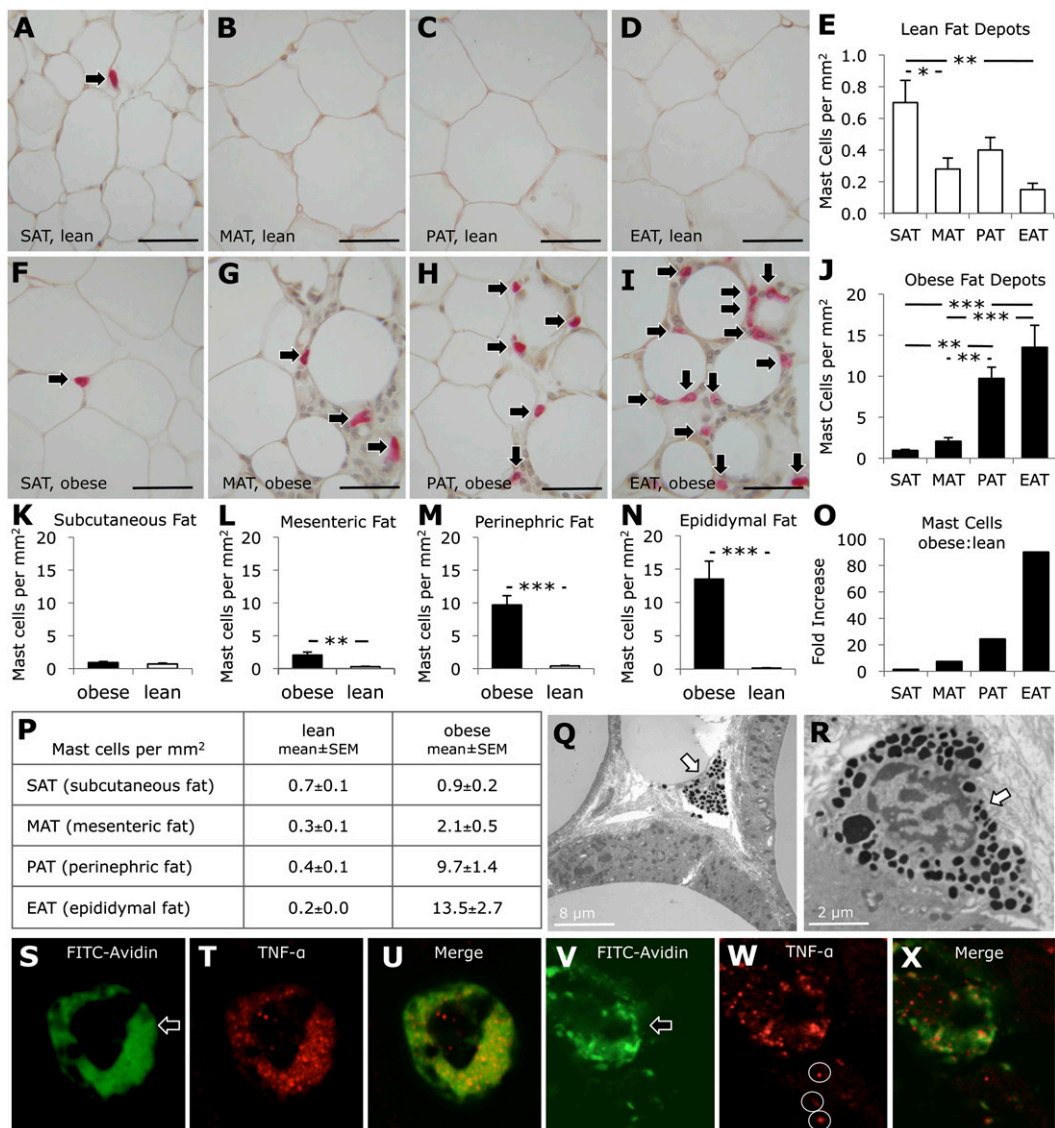


Fig. 3. Distribution of mast cells in abdominal fat depots. The densities of mast cells were determined in subcutaneous (SAT), mesenteric (MAT), perinephric (PAT), and epididymal (EAT) adipose tissues of lean (□) and obese (■) mice (A-P). In lean mice, subcutaneous adipose tissue contained more mast cells than visceral adipose tissues (A-E). In obese mice, however, mast cells were more prevalent in visceral adipose tissues (F-J). Whereas no significant change in mast cell density of subcutaneous adipose tissue was observed (K), obesity was accompanied by a substantial increase in mast cells in mesenteric (L), perinephric (M), and epididymal (N) adipose tissues. The largest increase in mast cell density was seen in epididymal adipose tissue in obese mice (O, P). Ultrastructural examination demonstrated mast cells packed with membrane-bound electron-dense granules (Q, R). Confocal micrographs show a fluorescein-labeled mast cell containing TNF- α in the epididymal adipose tissue of an obese mouse (S-U). TNF- α was also present in extracellular granules (circles) adjacent to a degranulating mast cell (V-X). Scale bars: 50 μ m or as indicated. Data are expressed as mean \pm SEM. * P < 0.05, ** P < 0.01, *** P < 0.001. TNF- α , tumor necrosis factor α .

CLS were distributed differentially in abdominal fat depots

CLS were found in all four abdominal fat depots in lean and obese mice (Fig. 5). Their density, however, differed from one depot to another (Fig. 5A-J). In lean mice, the lowest density of CLS was observed in subcutaneous fat depot (Fig. 5A-E). CLS were, for example, 7-fold less prevalent in subcutaneous than in perinephric fat depot (P < 0.01). Of note, CLS and solitary ATM had a similar distribution pattern in abdominal fat depots in lean mice (Figs.

5E, 4E). In obese mice, CLS were also less prevalent in subcutaneous than in visceral fat (Fig. 5F-J). In visceral fat depots in obese mice, the highest density of CLS was found in epididymal, followed by perinephric and mesenteric fat depots (Fig. 5G-J). Although obesity was accompanied by a substantial increase in CLS in all fat depots, subcutaneous fat depot had the lowest increase (Fig. 5K-P). The increase was 138-fold for epididymal, 49-fold for mesenteric, 43-fold for perinephric, and 14-fold for subcutaneous fat depot (Fig. 5O). In obese mice, CLS and mast cells had a

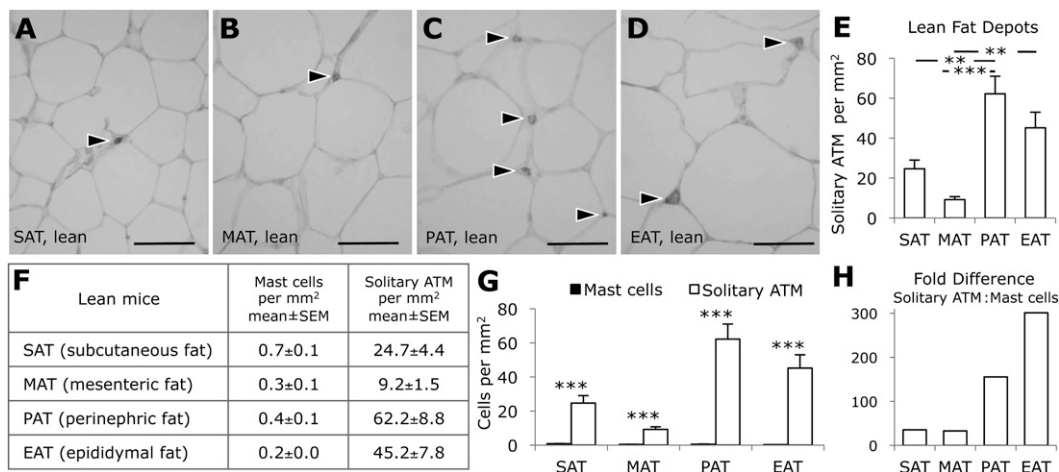


Fig. 4. Distribution of solitary ATM in abdominal fat depots. In lean C57BL/6 mice, solitary ATM were distributed differentially in abdominal fat depots (A-E). Solitary ATM were less prevalent in subcutaneous (SAT) than perinephric (PAT) and epididymal (EAT) adipose tissues (E-F). Solitary ATM were far more abundant than mast cells in all four abdominal fat depots examined (F-H). Scale bars: 50 μ m. Data are expressed as mean \pm SEM. ** $P < 0.01$, *** $P < 0.001$. ATM, adipose tissue macrophages.

similar distribution pattern in abdominal fat depots of obese mice (Figs. 5J, 3J). Ultrastructural examination demonstrated adipocytes with narrow cytoplasmic rims surrounding lipid cores in lean mice (Fig. 5Q). In obese mice, however, macrophages and mast cells enveloped some adipocytes forming CLS (Fig. 5R). On higher magnification, many macrophages and mast cells were found abutting on lipid cores with no evidence of the cytoplasm of adipocytes (Fig. 5S, T).

DISCUSSION

With an epidemic of global proportions, obesity and insulin-resistant diabetes have become health issues of major concern. Although adiposity affects many fat depots throughout the body, fat accumulation in visceral depots is closely linked to insulin resistance and adverse cardiovascular outcome. Recent evidence has shed light on biological diversity of fat found in different anatomical locations (24–26). Subcutaneous and visceral fat, for example, differ in insulin responsiveness, lipolysis, and glucose transporters. In the present study, we showed that subcutaneous and visceral fat also differ in immune cell composition and adipocyte turnover both in lean and DIO mice.

Although much attention has been focused on inflammatory changes present in adipose tissues in obesity, little is known about immune cell composition and adipocyte turnover of various fat depots in the lean state. In the present study, we showed that solitary ATM were prevalent in abdominal fat depots of lean mice. Our finding of a lower density of solitary ATM in subcutaneous fat is consistent with a lower macrophage content of subcutaneous versus omental fat reported in lean human subjects (32). With respect to biological significance, it is important to note that macrophages have a remarkable functional heterogeneity (33). It has been proposed that, by producing IL-10, alternatively activated macrophages in lean adipose tissues

create an anti-inflammatory milieu protecting adipocytes (34). Considering differences in biological behavior of fat found in different depots, it is conceivable that macrophages found in various fat depots have different functions. However, if this is not the case, a lower macrophage density in subcutaneous fat depot might reflect a lesser requirement for protective immunity in a fat depot that has a metabolically favorable phenotype.

The number of adipocytes in humans increases during childhood and adolescence and remains constant during adulthood (35). Adipocytes in adult humans have an annual renewal rate of about 10% (35). Although recent reports have demonstrated increased numbers of CLS, surrogates for dead adipocytes, in obese rodents and humans (7–9, 36), comparative analysis of adipocyte death rate in abdominal fat depots of lean subjects is lacking. In the present study, we showed that in lean mice perinephric fat had the highest and subcutaneous fat the lowest prevalence of CLS. Assuming a relatively steady weight for fat depots of six-month old adult mice, it could be argued that the highest rate of adipocyte turnover in abdominal fat depots of lean mice occurs in perinephric and the lowest in subcutaneous fat. In other words, adipocytes in subcutaneous depot appear to have a longer lifespan. We also showed that in lean mice the densities of solitary ATM correlated with those of CLS. Whereas the highest density of solitary ATM and CLS were found in perinephric fat, subcutaneous fat had the lowest density of CLS and a low density of solitary ATM. These findings suggest that metabolically healthy subcutaneous fat with a lower adipocyte turnover requires less immune surveillance provided by macrophages.

Consistent with recent reports (7–9, 36), we found a substantial increase in the prevalence of CLS in obese mice. Although the mechanisms underlying adipocyte injury and death are under investigation, it has been proposed that exaggerated metabolic demands owing to nutrient

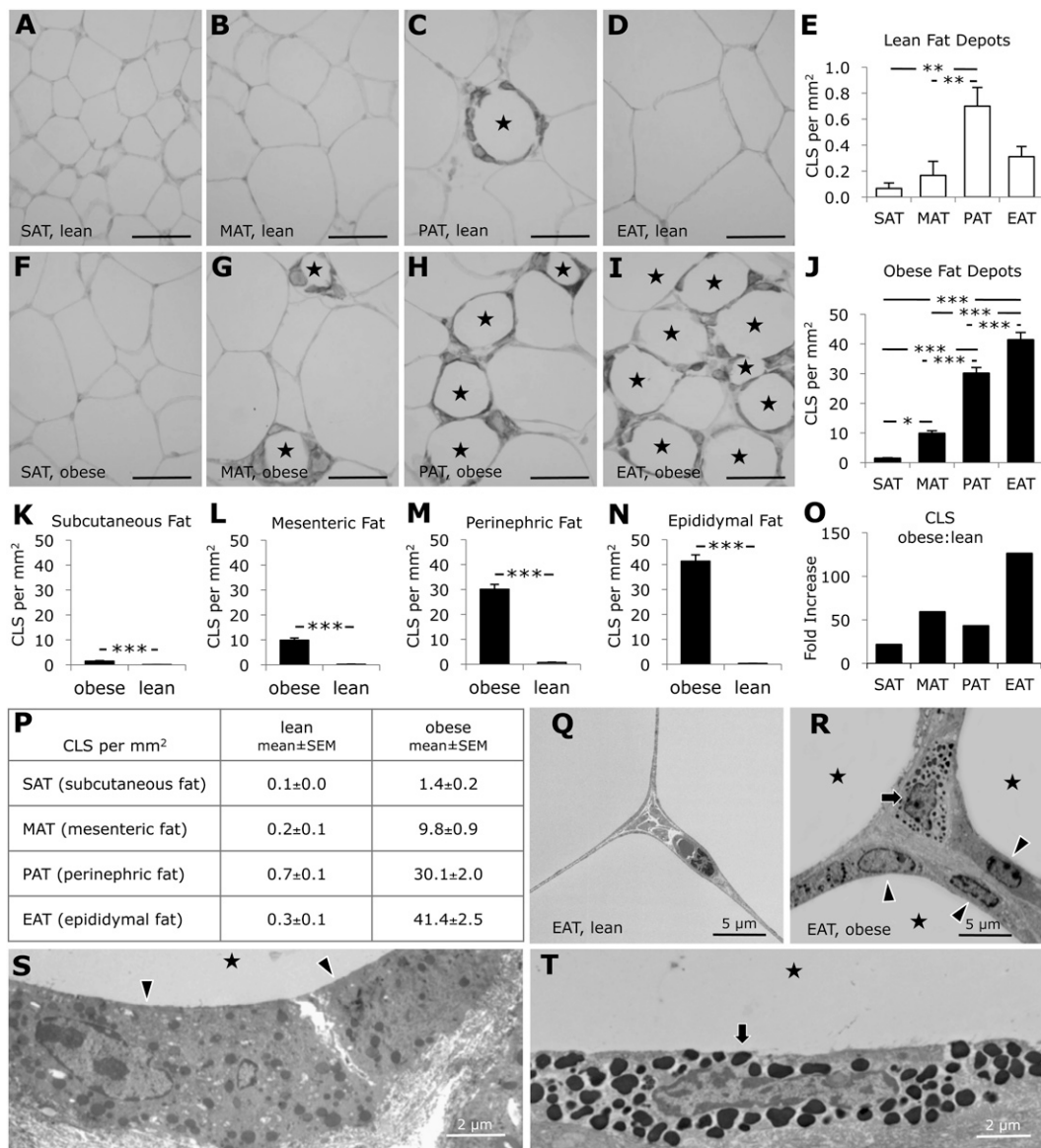


Fig. 5. Distribution of CLS in abdominal fat depots. CLS (stars) were distributed differentially in subcutaneous (SAT), mesenteric (MAT), perinephric (PAT), and epididymal (EAT) adipose tissues of lean (□) and obese (■) mice (A–J). In both lean and obese mice, subcutaneous adipose tissue had the lowest prevalence of CLS (A–J). Obesity was accompanied by a substantial increase in the density of CLS in subcutaneous (K), mesenteric (L), perinephric (M), and epididymal (N) fat depots. Ultrastructural examination demonstrated adipocytes with narrow cytoplasmic rims surrounding lipid cores in lean mice (Q). In obese mice, however, macrophages (arrowheads) and mast cells (arrow) enveloped adipocytes forming CLS (stars) (R). On higher magnification, many macrophages (arrowheads) and mast cells (arrow) were found abutting on lipid cores with no evidence of the cytoplasm of adipocytes (S, T). Scale bars: 50 μ m or as indicated. Data are expressed as mean \pm SEM. * P < 0.05, ** P < 0.01, *** P < 0.001. CLS, crown-like structures.

surplus triggers stress responses in adipocytes that could lead to cell injury and death (37). Based on immunohistochemical and ultrastructural findings, it was proposed that most macrophages in white adipose tissues of obese mice and humans were localized to adipocytes that demonstrated morphological features of necrosis, but not apoptosis (7). This notion has been challenged by a recent report that showed increased adipocyte apoptosis in obese humans and DIO mice (38). Moreover, insulin-resistant lipodystrophic mice demonstrated increased apoptotic cell death in adipose tissues (39). While there is still an ac-

tive debate over the mechanisms underlying adipocyte injury and death observed in conditions associated with alterations in body fat mass and insulin resistance, in the present study we deliberately avoided terms that would indicate the death pathway(s) that might be involved. Instead, to explore the differences in the prevalence of dead adipocytes between different fat depots, we studied the distribution of CLS, surrogates for dead adipocytes. In both lean and DIO mice, subcutaneous fat depot differed from visceral adipose tissues by a substantially lower prevalence of CLS. This finding is consistent with the low prevalence of


CLS in subcutaneous fat compared with visceral fat in leptin-deficient ob/ob and leptin receptor-deficient db/db mice, two commonly used models of genetic obesity (9).

Mast cells are among the most evolutionary conserved cellular elements of the immune system (40). Widely distributed in vertebrates, mast cells are found at the interface between the organism and its environment (i.e., skin, respiratory system, and gastrointestinal tract) and in connective tissues, especially in vicinity to blood vessels (41). To recognize and eliminate pathogens, mast cells possess a multitude of receptor systems and are capable of releasing mediators with antimicrobial, vasoactive, enzymatic, anticoagulant, and pro-inflammatory properties (17). In the present study, we showed that mast cells were more prevalent in subcutaneous than visceral fat of lean mice. Of note, large numbers of mast cells are also found in the skin of mice and humans (42–44). Considering the barrier function of the skin and the close proximity of subcutaneous fat to the skin, it could be argued that mast cells in subcutaneous fat provide support to the skin immune system (45). Alternatively, considering their functional versatility (46), mast cells in subcutaneous fat might have anti-inflammatory functions and contribute to the suppression of inflammatory signals arising in the microenvironment.

A recent study showed ~5-fold increase in the numbers of mast cells in “white adipose tissue” of DIO mice (16). Although the report does not specify what fat depot this is referred to, the increase in adipose tissue mast cells in obesity is consistent with the findings in the present study. However, in the present study, we found significantly more mast cells (≤ 90 -fold) in visceral fat of obese compared with lean mice. The observed differences between studies is likely related to the higher fat content of the diet and the longer duration of high-fat feeding in the present study. Once again, we found that subcutaneous fat behaved very differently from visceral fat in that obesity was accompanied by only a modest increase (31%) in mast cell density of subcutaneous fat.

As mentioned above, TNF- α was found to be upregulated in visceral fat of obese rodents and neutralization of TNF- α alleviated insulin resistance (3). Considering that certain mast cells are capable of storing and secreting TNF- α (47), we asked whether adipose tissue mast cells of obese mice contain TNF- α . We found that a significant number of mast cells in epididymal fat of obese mice express TNF- α . Moreover, we found that some mast cells were in the process of degranulation and that TNF- α was present in the granules in the adjacent interstitium. Therefore, by secreting TNF- α , mast cells in visceral fat of obese mice contribute to local and systemic insulin resistance.

In conclusion, we found that mast cells, solitary ATM, and CLS were distributed differentially in abdominal fat depots of lean and DIO mice. Subcutaneous fat differed from visceral fat by immune cell composition and a lower prevalence of CLS both in lean and obese mice. A substantial rise in the density of mast cells in visceral fat of obese mice suggests a role for mast cells in the pathogenesis of obesity and insulin resistance. A better understanding of

underlying mechanisms will help identify targets of therapeutic significance. 

The authors express their gratitude to Armando Mendez (Diabetes Research Institute, University of Miami) for critically reviewing the manuscript.

REFERENCES

1. Mokdad, A. H., E. S. Ford, B. A. Bowman, W. H. Dietz, F. Vinicor, V. S. Bales, and J. S. Marks. 2003. Prevalence of obesity, diabetes, and obesity-related health risk factors, 2001. *JAMA*. **289**: 76–79.
2. Hotamisligil, G. S. 2006. Inflammation and metabolic disorders. *Nature*. **444**: 860–867.
3. Hotamisligil, G. S., N. S. Shargill, and B. M. Spiegelman. 1993. Adipose expression of tumor necrosis factor- α : direct role in obesity-linked insulin resistance. *Science*. **259**: 87–91.
4. Uysal, K. T., S. M. Wiesbrock, M. W. Marino, and G. S. Hotamisligil. 1997. Protection from obesity-induced insulin resistance in mice lacking TNF- α function. *Nature*. **389**: 610–614.
5. Xu, H., G. T. Barnes, Q. Yang, G. Tan, D. Yang, C. J. Chou, J. Sole, A. Nichols, J. S. Ross, L. A. Tartaglia, et al. 2003. Chronic inflammation in fat plays a crucial role in the development of obesity-related insulin resistance. *J. Clin. Invest.* **112**: 1821–1830.
6. Weisberg, S. P., D. McCann, M. Desai, M. Rosenbaum, R. L. Leibel, and A. W. Ferrante, Jr. 2003. Obesity is associated with macrophage accumulation in adipose tissue. *J. Clin. Invest.* **112**: 1796–1808.
7. Cinti, S., G. Mitchell, G. Barbatelli, I. Murano, E. Ceresi, E. Faloia, S. Wang, M. Fortier, A. S. Greenberg, and M. S. Obin. 2005. Adipocyte death defines macrophage localization and function in adipose tissue of obese mice and humans. *J. Lipid Res.* **46**: 2347–2355.
8. Nayer, A., and S. E. Shoelson. 2007. Differential distribution of adipositis induced by high-fat diet in abdominal fat depots. *Diabetes*. **56** (Suppl. 1): 272-OR.
9. Murano, I., G. Barbatelli, V. Parisani, C. Latini, G. Muzzonigro, M. Castellucci, and S. Cinti. 2008. Dead adipocytes, detected as crown-like structures, are prevalent in visceral fat depots of genetically obese mice. *J. Lipid Res.* **49**: 1562–1568.
10. Nathan, C. 2002. Points of control in inflammation. *Nature*. **420**: 846–852.
11. Feuerer, M., L. Herrero, D. Cipolletta, A. Naaz, J. Wong, A. Nayer, J. Lee, A. B. Goldfine, C. Benoist, S. Shoelson, et al. 2009. Lean, but not obese, fat is enriched for a unique population of regulatory T cells that affect metabolic parameters. *Nat. Med.* **15**: 930–939.
12. Nishimura, S., I. Manabe, M. Nagasaki, K. Eto, H. Yamashita, M. Ohsugi, M. Otsu, K. Hara, K. Ueki, K. Sugiura, et al. 2009. CD8+ effector T cells contribute to macrophage recruitment and adipose tissue inflammation in obesity. *Nat. Med.* **15**: 914–920.
13. Ohmura, K., N. Ishimori, Y. Ohmura, S. Tokuhara, A. Nozawa, S. Horii, Y. Andoh, S. Fujii, K. Iwabuchi, K. Onoé, et al. 2010. Natural killer T cells are involved in adipose tissues inflammation and glucose intolerance in diet-induced obese mice. *Arterioscler. Thromb. Vasc. Biol.* **30**: 193–199.
14. Hellman, B. 1965. Studies in obese-hyperglycemic mice. *Ann. N. Y. Acad. Sci.* **131**: 541–558.
15. Hristova, M., L. Aloe, P. I. Ghenev, M. Fiore, and G. N. Chaldakov. 2001. Leptin and mast cells: a novel adipoimmune link. *Turk. J. Med. Sci.* **31**: 581–583.
16. Liu, J., A. Divoux, J. Sun, J. Zhang, K. Clément, J. N. Glickman, G. K. Sukhova, P. J. Wolters, J. Du, C. Z. Gorgun, et al. 2009. Genetic deficiency and pharmacological stabilization of mast cells reduce diet-induced obesity and diabetes in mice. *Nat. Med.* **15**: 940–945.
17. Marshall, J. S. Mast-cell responses to pathogens. 2004. *Nat. Rev. Immunol.* **4**: 787–799.
18. Mota, I., and I. Vugman. 1956. Effects of anaphylactic shock and compound 48/80 on the mast cells of the guinea pig lung. *Nature*. **177**: 427–429.
19. Wintroub, B. U., M. C. Mihm, Jr., E. J. Goetzl, N. A. Soter, and K. F. Austen. 1978. Morphologic and functional evidence for release of mast-cell products in bullous pemphigoid. *N. Engl. J. Med.* **298**: 417–421.

20. Secor, V. H., W. E. Secor, C. A. Gutekunst, and M. A. Brown. 2000. Mast cells are essential for early onset and severe disease in a murine model of multiple sclerosis. *J. Exp. Med.* **191**: 813–822.
21. Lee, D. M., D. S. Friend, M. F. Gurish, C. Benoist, D. Mathis, and M. B. Brenner. 2002. Mast cells: a cellular link between autoantibodies and inflammatory arthritis. *Science*. **297**: 1689–1692.
22. Sun, J., G. K. Sukhova, P. J. Wolters, M. Yang, S. Kitamoto, P. Libby, L. A. MacFarlane, J. Mallen-St Clair, and G. P. Shi. 2007. Mast cells promote atherosclerosis by releasing proinflammatory cytokines. *Nat. Med.* **13**: 719–724.
23. Trayhurn, P. 2005. Endocrine and signalling role of adipose tissue: new perspectives on fat. *Acta Physiol. Scand.* **184**: 285–293.
24. Kissebah, A. H., and G. R. Krakower. 1994. Regional adiposity and morbidity. *Physiol. Rev.* **74**: 761–811.
25. Wajchenberg, B. L. 2000. Subcutaneous and visceral adipose tissue: their relation to the metabolic syndrome. *Endocr. Rev.* **21**: 697–738.
26. Giorgino, F., L. Laviola, and J. W. Eriksson. 2005. Regional differences of insulin action in adipose tissue: insights from in vivo and in vitro studies. *Acta Physiol. Scand.* **183**: 13–30.
27. Riley, J. F., and G. B. West. 1955. Tissue mast cells: studies with a histamine-liberator of low toxicity (compound 48/80). *J. Pathol. Bacteriol.* **69**: 269–282.
28. Leder, L. D. 1964. On the selective enzyme-cytochemical demonstration of neutrophilic myeloid cells and tissue mast cells in paraffin sections. *Klin. Wochenschr.* **42**: 553.
29. Tharp, M. D., L. L. Seelig, Jr., R. E. Tigelaar, and P. R. Bergstresser. 1985. Conjugated avidin binds to mast cell granules. *J. Histochem. Cytochem.* **33**: 27–32.
30. Combs, J. W. 1971. An electron microscope study of mouse mast cells arising in vivo and in vitro. *J. Cell Biol.* **48**: 676–684.
31. Austyn, J. M., and S. Gordon. 1981. F4/80, a monoclonal antibody directed specifically against the mouse macrophage. *Eur. J. Immunol.* **11**: 805–815.
32. Harman-Boehm, I., M. Blüher, H. Redel, N. Sion-Vardy, S. Ovadia, E. Avinoach, I. Shai, N. Klötting, M. Stumvoll, N. Bashan, et al. 2007. Macrophage infiltration into omental versus subcutaneous fat across different populations: effect of regional adiposity and the comorbidities of obesity. *J. Clin. Endocrinol. Metab.* **92**: 2240–2247.
33. Gordon, S., and P. R. Taylor. 2005. Monocyte and macrophage heterogeneity. *Nat. Rev. Immunol.* **5**: 953–964.
34. Lumeng, C. N., J. L. Bodzin, and A. R. Saltiel. 2007. Obesity induces a phenotypic switch in adipose tissue macrophage polarization. *J. Clin. Invest.* **117**: 175–184.
35. Spalding, K. L., E. Arner, P. O. Westermark, S. Bernard, B. A. Buchholz, O. Bergmann, L. Blomqvist, J. Hoffstedt, E. Näslund, T. Britton, et al. 2008. Dynamics of fat cell turnover in humans. *Nature*. **453**: 783–787.
36. Strissel, K. J., Z. Stancheva, H. Miyoshi, J. W. Perfield 2nd, J. DeFuria, Z. Jick, A. S. Greenberg, and M. S. Obin. 2007. Adipocyte death, adipose tissue remodeling, and obesity complications. *Diabetes*. **56**: 2910–2918.
37. Ozcan, U., Q. Cao, E. Yilmaz, A. H. Lee, N. N. Iwakoshi, E. Ozdelen, G. Tuncman, C. Görgün, L. H. Glimcher, and G. S. Hotamisligil. 2004. Endoplasmic reticulum stress links obesity, insulin action, and type 2 diabetes. *Science*. **306**: 457–461.
38. Alkhoury, N., A. Gornicka, M. P. Berk, S. Thapaliya, L. J. Dixon, S. Kashyap, P. R. Schauer, and A. E. Feldstein. 2010. Adipocyte apoptosis, a link between obesity, insulin resistance, and hepatic steatosis. *J. Biol. Chem.* **285**: 3428–3438.
39. Herrero, L., H. Shapiro, A. Nayer, J. Lee, and S. E. Shoelson. 2010. Inflammation and adipose tissue macrophages in lipodystrophic mice. *Proc. Natl. Acad. Sci. USA*. **107**: 240–245.
40. Hardy, W. B. 1892. The blood-corpuscles of the crustacea, together with a suggestion as to the origin of the crustacean fibrin-ferment: part I. *J. Physiol.* **13**: 165–190.
41. Chiu, H., and D. Lagunoff. 1972. Histochemical comparison of vertebrate mast cells. *Histochem. J.* **4**: 135–144.
42. Majeed, S. K. 1994. Mast cell distribution in mice. *Arzneimittelforschung*. **44**: 1170–1173.
43. Gersch, C., O. Dewald, M. Zoerlein, L. H. Michael, M. L. Entman, and N. G. Frangogiannis. 2002. Mast cells and macrophages in normal C57/BL/6 mice. *Histochem. Cell Biol.* **118**: 41–49.
44. Weidner, N., and K. F. Austen. 1990. Evidence for morphologic diversity of human mast cells. An ultrastructural study of mast cells from multiple body sites. *Lab. Invest.* **63**: 63–72.
45. Metz, M., F. Siebenhaar, and M. Maurer. 2008. Mast cell functions in the innate skin immune system. *Immunobiology*. **213**: 251–260.
46. Galli, S. J., M. Grimaldeston, and M. Tsai. 2008. Immunomodulatory mast cells: negative, as well as positive, regulators of immunity. *Nat. Rev. Immunol.* **8**: 478–486.
47. Gordon, J. R., and S. J. Galli. 1990. Mast cells as a source of both preformed and immunologically inducible TNF-alpha/cachectin. *Nature*. **346**: 274–276.